Regular Article

PHYSICAL CHEMISTRY RESEARCH
Published by the
Iranian Chemical Society
www.physchemres.org
info@physchemres.org

Phys. Chem. Res., Vol. 8, No. 3, 457-469, September 2020
DOI: 10.22036/pcr.2020.211251.1706

Quantum Chemical and Molecular Docking Studies of Imidazole and Its Derivatives as the Active Antifungal Components against C. Albicans

S. Slassi[a], H. Zaki[b], A. Amine[a], K. Yamni[a] and M. Bouachrine[c,d,*]

[a]*LCBAE laboratory, CMMB, Faculty of Science, Moulay Ismail University, Meknes, Morocco*
[b]*BEH Laboratory, Faculty of Science and Technics, Moulay Ismail University, Errachidia, Morocco*
[c]*MCNS laboratory, CMC, Faculty of Science, Moulay Ismail University, Meknes, Morocco*
[d]*MEM, ESTM, Moulay Ismail University, Meknes, Morocco*

(Received 9 December 2019, Accepted 22 April 2020)

Heterocyclic compounds of imidazole have been extensively studied because they are promising for pharmaceuticals applications and synthetic chemistry. Thus, the synthesis, characterization, and optical properties of four different Schiff base ligands based on imidazole named L1-L4 have been the subject of many recent studies. The antifungal properties of these compounds on an important pathogenic fungal species (Candida albicans) have been also studies. In this study, at first, quantum chemical calculations, in the framework of density functional theory, were performed on four imidazole-based structures (L1, L2, L3 and L4) to determine their structural and electronic properties and to understand the correlation between their structures and properties. In the second part, the molecular docking was carried out on the most and the least active compounds (L1 and L4) with their targeted proteins to explain the origin of these in silico antioxidant properties and to examine the probable binding modes of the studied compounds with the corresponding amino acid residues of protein. The theoretical results are also compared with experimental data.

Keywords: Imidazole, Candida albicans, Molecular docking, Binding mode

INTTRODUCTION

Imidazole-based organic compounds are among the main precursors of synthetic intermediates and pharmaceuticals [1-4]. Imidazole consists of a five-member hetero-aromatic ring with two nitrogen atoms. In nature, imidazole is found in many natural products possessing various biological activities and also present in the human organisms, such as the histidine amino acid, a component of DNA base structure [5].

Heterocyclic compounds of imidazole have been extensively studied because they are promising for pharmaceuticals applications, synthetic chemistry and biochemical processes [6-7]. These compounds are well-known for their biological and especially pharmacological activities as antitumor, anti HIV, antimicrobial, anticonvulsant, antioxidant, antihypertensive, anticancer, analgesic, anti-inflammatory, antimicrobial, antidepressant, cytotoxic, analgesic, anti-HIV, antileishmanial, anticonvulsant, anti-inflammatory and anticancer [8-11].

Apart from biological applications, these molecules have interesting corrosion properties as potential inhibitors for transition metals [12], optoelectronic applications (OLED) [13] and non-linear optic (NLO) systems [14]. The excellent properties of imidazole and its derivatives can be attributed to, first, their aromatic nature, second, the presence of heteroatom and a pi-conjugated system, and, third, the hydrogen bond donor-acceptor, Van der Waals, pi staking, hydrophobic interactions as well as their high affinity for metals. Thus, four different Schiff base ligands named L1, L2, L3 and L4 (Fig. 1) have been prepared and characterized by S. Slassi *et al.* [15].

*Corresponding author. E-mail: m.bouachrine@umi.ac.ma

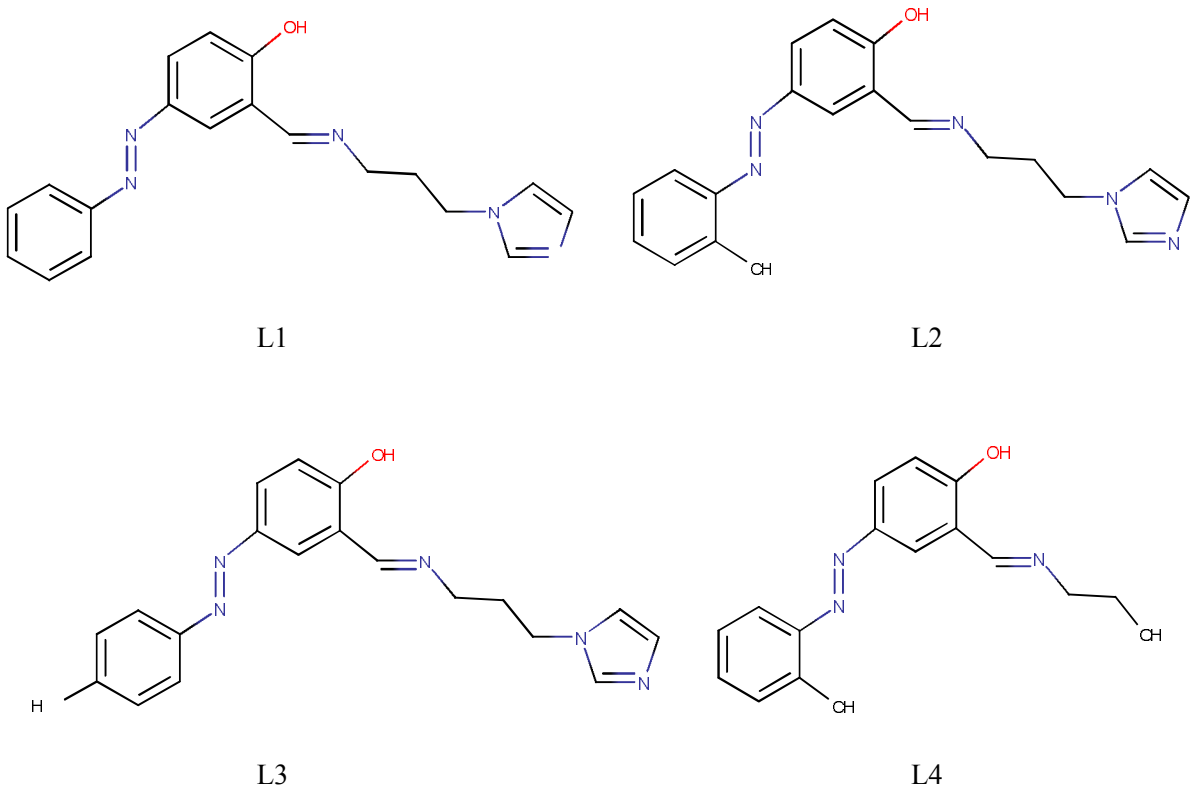

Fig. 1. Four ligands containing imidazole compounds (L1, L2, L3 and L4).

According to these authors, the synthesized ligands can be used in many applications in the biological and pharmaceutical fields since they possess interesting antifungal properties on an important pathogenic fungal species, Candida albicans. These species cause nosocomial infections through the infection of the bloodstream [16,17]. Despite the scientific progress, especially in developing the antifungal drugs, the number of patients with this disease has increased considerably in recent years [18]. We are interested in the structural study of these molecular systems and the different interactions between these molecules and the corresponding receptors using computational tools, especially quantum chemical calculations and molecular docking. It is worth noting that the quantum chemical methods based on density functional theory (DFT) coupled with experimental techniques play crucial role in studying several physico-chemical properties of organic molecules. The hybrid functional, B3LYP [19] is most widely used because it offers low computational cost and commonly excellent results. Herein, we use DFT-based quantum chemical calculations at the B3LYP-D3/6-31G(d,p) level of theory to study the molecular geometry. Then, the molecular docking is performed in order to explain in silico antioxidant properties and to investigate the possible binding sites and different interactions between the Li ligands and the amino acids resulting from the corresponding proteins. The results of molecular docking as well as those of quantum studies are then compared with experimental data.

MATERIALS AND METHODS

Data Set

The chemical data with their reported antifungal properties and antioxidant activities were taken from literature [15]. Antifungal activities of the compounds L1 to L4 were evaluated on an important fungal species which is pathogenic for humans: Candida albicans

Table 1. Antifungal Activities Obtained in a Solid Medium (nm) [15]

Studied compounds	L1	L2	L3	L4
C. Albicans	17	14.5	14.5	12.5

Table 2. Antifungal Activities Obtained in a Liquid Medium (mg ml^{-1}) [15]

Studied compounds	L1	L2	L3	L4
C. Albicans	0.8	0.1	0.2	3

implicated in patients with cystic fibrosis [20]. According to the authors, the activities were determined by rapid antifungal screening using a disc diffusion method in a solid medium; the antifungal activity values are listed with their corresponding structures in Tables 1 and 2.

DFT Calculations

In this study, the Becke's hybrid functional with three parameters B3 and the nonlocal correlation of Lee-Yang-Parr LYP, called B3LYP method, was used [19]. The 6-31G(d,p) basis set was used for all calculations [21]. The DFT were performed using the Gaussian 09 package [22]. It is noted that the use of this method as well as this basis set appears to be adequate approach for the study of physico-chemical properties of these compounds and most organic compounds [23-29]. This method introduces electron correlation effects at a lower cost in the computation's time. The geometry structures of the neutral molecules (L1, L2, L3 and L4) were optimized under no constraint. We also determined the highest occupied molecular orbital (HOMO) and the lowest unoccupied molecular orbital (LUMO) levels of the target molecules. The E_{gap} energy, as the energy difference between the energy levels of HOMO and LUMO, and other electronic parameters were also calculated.

Molecular Docking

Molecular docking was performed to examine the type of interactions between the studied compounds shown in Fig. 1 and the protein to validate the experimental results. The compounds and protein preparation steps for the docking protocol were carried out in Autodock tools 1.5.4 from MGL Tools package using default parameters [30]. A grid box (x = 67.5, y = 69.2, z = 3.64 at 1 Å spacing) was set to cover the tetrazole-based antifungal drug candidate binding site in the studied enzyme Candida albicans sterol 14 alpha-demethylase (CYP51). The bioactive conformations were simulated using Autodock Vina [31]. The results were analyzed using Discovery Studio 2016 [32] software. The crystal structure of the enzyme (PDB entry code: 5TZ1) [33] was downloaded from the protein data bank (http://www.rcsb.org), and its original ligand was removed, then, the studied ligands in their DFT optimized conformation (compounds: L1, L2, L3 and L4) from our data set were docked in the active site of the studied enzyme (5TZ1). The PDB file was prepared using Discovery Studio 2016 cofactors and solvent molecules were removed from the model. For docking study, the three-dimensional structures of ligands were built and optimized using DFT method by the parameters described before on the software Gaussian 09.

RESULTS AND DISCUSSION

DFT Results

In order to theoretically characterize the molecules under study, to determine their structural and electronic properties and to understand the correlation existing between the structures and properties, all the structures were optimized at the B3LYP/6-31G(d,p) level. The optimized geometries of molecules L1, L2, L3 and L4 are shown

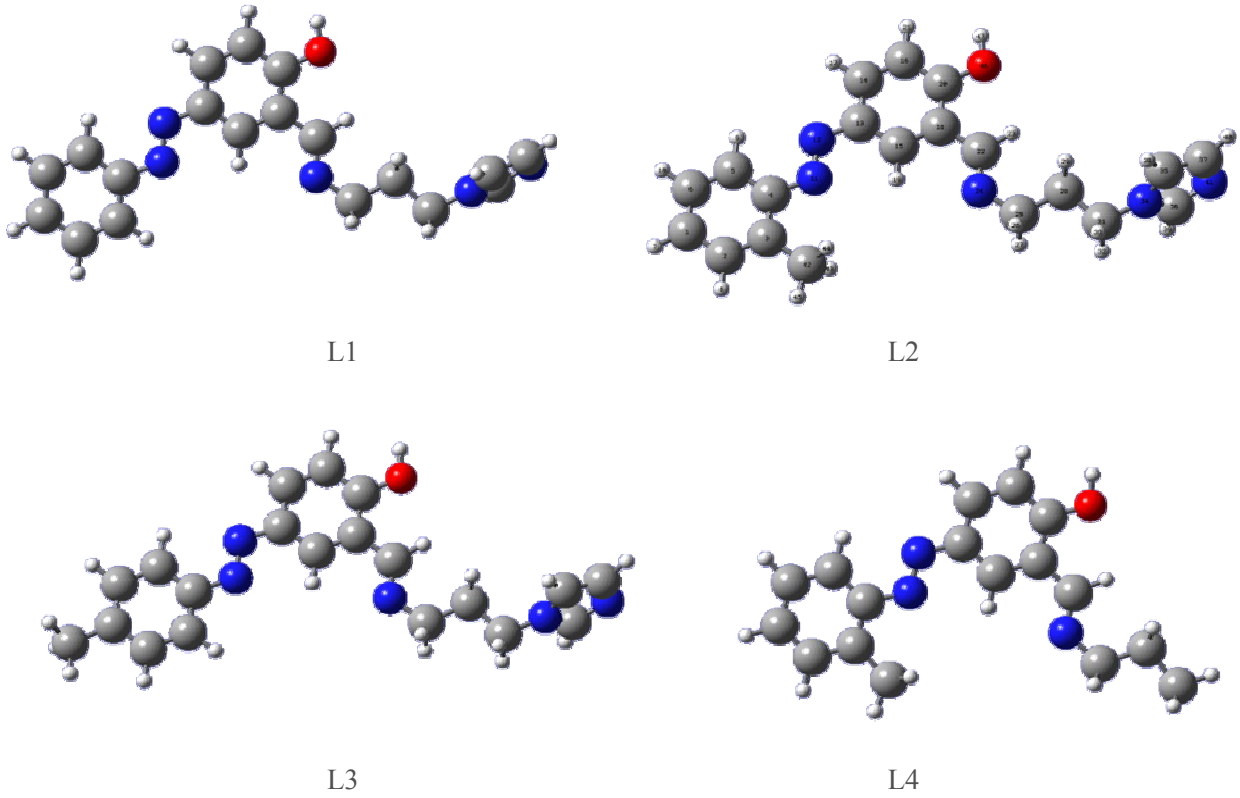

Fig. 2. Optimized geometries of the compounds L1, L2, L3 and L4.

in Fig. 2

Based on the results shown in Table 3, the bond lengths and angles obtained agree well with the experimental X-ray crystal data for the compound L2 [34]. The difference between the theoretical and experimental results can be attributed to the isolated molecules in the gas phase in DFT calculations, whereas the experimental properties are in the solid state.

The electron distribution in HOMOs and LUMOs reflect the chemical stability and the reactivity of the compounds. The properties of these occupied and unoccupied orbitals make it possible to predict the most reactive sites and to explain the reaction mechanisms. It also gives information about the properties of the molecules under study and their interactions with biological receptor. Experimentally, the energies of HOMO and LUMO are obtained through the electrochemical potential of oxidation and reduction reactions. Theoretically, these properties are also accessible by quantum calculation using DFT. The HOMO indicates the character of electron-donation, or the ability to donate an electron, while the LUMO indicates the character of electron-acceptation or the ability to obtain an electron.

In Fig. 3, the orbital lobes of HOMO and LUMO of our compounds are shown. We note that these orbitals have similar electronic distributions regardless of the compound under study. The electron distribution of HOMOs of all compounds is localized on the whole molecule and presents the anti-bonding character between the two adjacent fragments; whereas, the electron distribution of LUMOs is mainly localized on the conjugated bridge and presents the bonding character between the two adjacent fragments.

On the other hand, the energy gap is an interesting parameter that can explain different electronic properties, and stability of any compound. The small band gap facilitates the transfer of electrons from HOMO level to LUMO level when the material absorbs the wavelength light, while the large band gap reflects low reactivity and high stability. Therefore, the energies of HOMO, LUMO

Table 3. Geometrical Parameters of the Compounds L1, L2, L3 and L4: Bond (Å) and Bond Angle (°)

	Exp (L2)	B3LYP (L2)	B3LYP (L1)	B3LYP (L3)	B3LYP (L4)
C1-C2	1.376	1.392	1.383	1.394	1.394
C1-H7	0.93	1.100	1.076	1.086	1.086
C2-C3	1.392	1.399	1.391	1.400	1.400
C3-C42	1.504	1.462	1.511	1.509	1.509
C4-C5	1.389	1.409	1.392	1.405	1.405
C5-C6	1.377	1.391	1.380	1.388	1.388
C6-C1	1.37	1.393	1.387	1.399	1.399
C5-H9	0.93	1.102	1.073	1.084	1.084
C4-N11	1.439	1.437	1.421	1.417	1.417
N11-N12	1.24	1.231	1.220	1.262	1.262
N12-C13	1.421	1.438	1.417	1.414	1.414
C13-C14	1.395	1.412	1.385	1.401	1.403
C14-C16	1.372	1.388	1.381	1.388	1.388
C14-H17	0.93	1.103	1.075	1.085	1.085
C20-O46	1.338	1.374	1.349	1.364	1.365
C16-C20	1.396	1.403	1.386	1.399	1.399
C16-H21	0.93	1.1	1.077	1.088	1.088
C18-C22	1.454	1.47	1.483	1.476	1.478
C22-N24	1.271	1.287	1.252	1.276	1.275
N24-C25	1.462	1.431	1.445	1.454	1.456
C25-C28	1.508	1.527	1.53	1.535	1.534
C25-H27	0.97	1.13	1.088	1.100	1.100
C28-C31	1.517	1.53	1.529	1.534	1.533
C31-N34	1.458	1.432	1.449	1.458	-
C31-H33	0.93	1.128	1.085	1.096	1.096
N34-C36	1.341	1.405	1.349	1.369	-
C37-N41	1.357	1.395	1.368	1.377	-

Table 3. Continued

C35-C37	1.353	1.407	1.351	1.373	-
C35-N34	1.361	1.399	1.372	1.382	-
C35-H38	0.93	1.087	1.069	1.080	-
C37-H40	0.93	1.089	1.070	1.081	-
C3-C4-N11	116.9	116.96	116.00	115.84	115.84
N11-N12-C13	115.98	119.71	115.90	115.03	115.06
C2-C3-C42	121.9	119.48	120.40	120.66	120.66
N12-C13-C14	114.4	115.64	115.77	115.44	115.44
C20-O46-H47	109.5	108.16	111.12	109.34	109.19
C18-C22-N24	120.7	122.90	121.40	121.26	121.26
N24-C25-C28	109.41	119.31	119.94	119.39	119.39
C31-N34-C36	126	126.82	126.93	126.80	-
C31-N34-C35	127.2	126.52	127.07	126.86	-
N34-C36-N41	112.1	111.34	112.90	112.52	-
N41-C37-H40	124.6	121.50	121.61	121.44	-

and gap energy were determined from the DFT optimized structures of the compounds (Table 4). We also calculated other chemical descriptors such as the ionization potential (I), the electron affinity (A), the chemical hardness (η) and the softness (ρ) according to Koopman's theorem [35-36].

The ionization potential (I): $I = - E_{HOMO;}$

The electron affinity (A): $A = - E_{LUMO;}$

The chemical hardness (η):

$$\eta = 1/2 (-A + I) = 1/2 (E_{LUMO} - E_{HOMO});$$

The softness (ρ): $\rho = 1/\eta$

It is known that the energy of HOMO (E_{HOMO}) indicates the tendency towards the electron donation while the energy of LUMO (E_{LUMO}) indicates the ability to accept electrons. Therefore, the obtained values of (E_{HOMO}, E_{LUMO}) are (-5.918, -2.104), (-5.852, -2.114), (-5.799, -2.026) and (-5.718, -1.991) for L1, L2, L3 and L4, respectively. The low value of the HOMO energy and the high value of the LUMO energy are probably responsible for the high activity of the L1 compound. This is in a good agreement with the experimental results suggesting the following order of experimental activities L1 > L2 > L3 > L4. Considering the value of the energy gap, ΔE, larger values of the energy difference reflect low reactivity and high stability. The band gap value of L2 indicates that this molecule has a stable structure. This is confirmed by the high hardness value and the low softness value obtained, indicating that the molecule L1 could have a better performance as a ligand.

Dipole moment, μ (Debye), is another important parameter that results from non-uniform distribution of charg on the various atoms in the molecule [37]. The high value of μ (Debye) probably increases the interaction between the molecule and the protein and increases the activity of the ligands studied. In our study, we calculated the dipole moment of the studied molecules. The obtained results show that the most active molecule L1 has a dipole

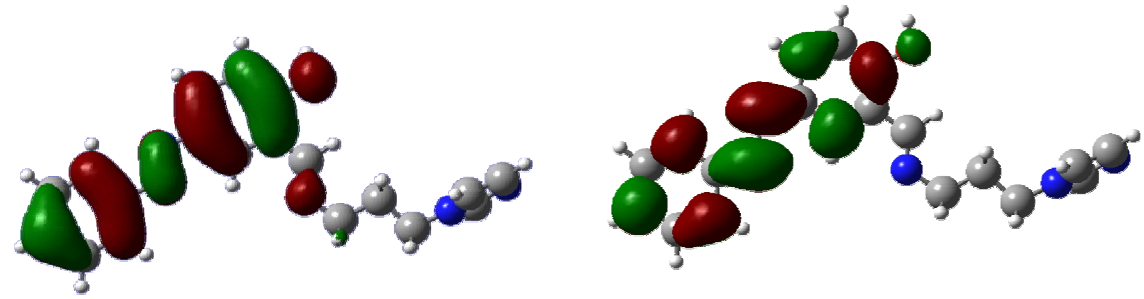

L1

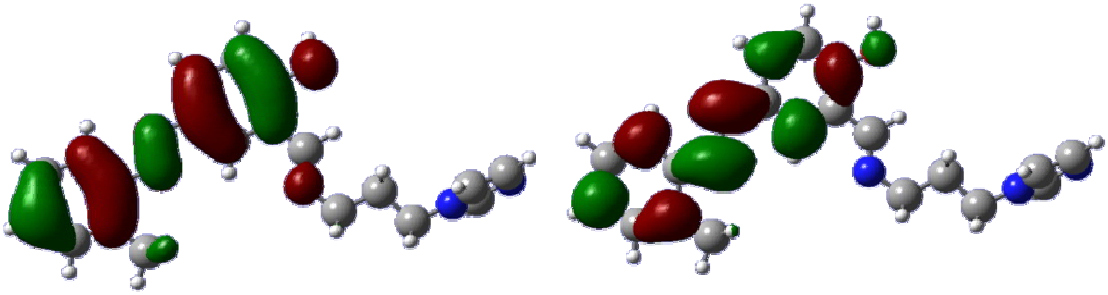

L2

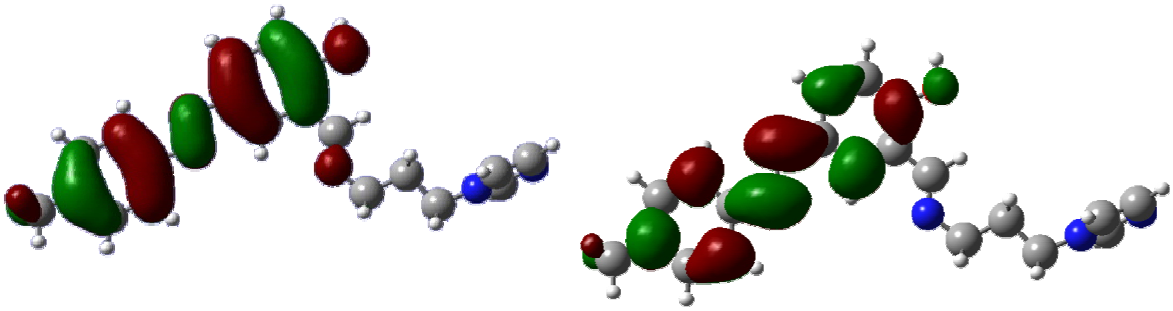

L3

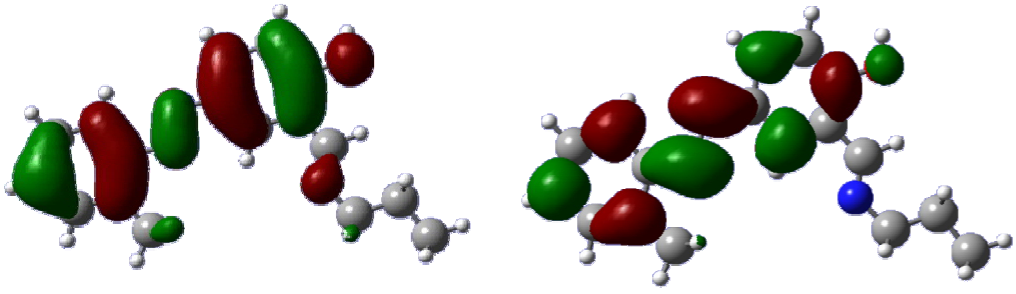

L4

Fig. 3. The DFT-based HOMO and LUMO molecular orbitals of the compounds L1-L4 at the B3LYP/6-31G(d,p) level.

Table 4. Quantum Chemical Parameters for the Compounds L1-L4 Obtained Using the DFT Approach at the B3LYP/6-31G(d,p) Level

	E_{HOMO} (eV)	E_{LUMO} (eV)	Egap (eV)	Hardness (η)	Softness (ρ)	Dipole moment, μ (Debye)
L1	-5.9189	-2.1043	3.8146	1.9073	0.5242	3.437
L2	-5.8522	-2.1141	3.7381	1.8690	0.5350	3.093
L3	-5.7994	-2.0267	3.7727	1.8863	0.5301	3.960
L4	-5.7185	-1.9916	3.7269	1.8634	0.5366	2.620

moment of the order of 3.437 D, a value superior to that obtained in the case of the least active molecule L4 (2.62 D).

Molecular Docking

The molecular docking analysis [36] was carried out for the compounds L1-L4 with their corresponding proteins. The crystal structure of the enzyme (PDB entry code: 5TZ1) was downloaded from the protein data bank (http://www.rcsb.org) and its original ligand was removed. The studied ligands in their DFT optimized conformation (compounds: L1, L2, L3 and L4) were docked in the active site of the enzyme. We searched an appropriate enzyme for our study, the sterol 14α-demethylase appears the best one because it is a cytochrome P450 enzyme involved in the conversion of lanosterol to 4,4-dimethylcholesta-8 (9), 14,24-triene-3β-ol [38]. These isoenzymes of cytochrome P450 are the main components in the biological synthesis of vitamins and lipids as well as the metabolism of organic substances [39]. As a member of this family, sterol 14α-demethylase is responsible for an essential step in the biosynthesis of ergosterol in fungi, which is a vital substance for the cell. It enters in the membrane structure and is an important element in the regulation of the fluidity and permeability of the membrane influencing the activity of enzymes, ion channels and other cellular components. We chose this enzyme to perform docking for the following reasons:

This enzyme has been reported in the literature as an antifungal therapeutic target by azoles to block sterol synthesis in *C. albicans* [40];

Many researchers have discussed the presence of the enzyme sterol-14-α-demethylase in fungi causing disruption of the plasma membrane accompanied by cell leakage and ultimately the death of the pathogen in (our case *C. albicans*), by destroying the ability of the fungal cell to produce ergosterol [41].

The interactions between the enzyme *Candida albicans* sterol 14 alpha-demethylase (CYP51) and the compounds studied here, L1 (the more active), L4 (the less active), are shown in Fig. 4.

The two compounds L1 and L4 show different types of interactions with the potential target sterol 14 alpha-demethylase, such as Electrostatic interactions, hydrogen bond, Pi-anion, hydrophobic interactions type Pi-Alkyl and Pi-sigma. Table 5 summarizes the different type and number of the interactions.

Figure 5a shows that the most active compound L1 presents:

03 pi-sigma interaction with PHE A:233, TYR A:118 and PHE A:436 residues, which can be seen in dark purple dotted lines,

02 strong hydrogen bonds, the first between the TYR A:132 residue and the oxygen of O-H bond and the second between hydrogen of N in the imine moiety and the hydrogen of the TYR A:132 residue, which can be seen in green dotted lines,

while the less active compound L4 presents:

01 conventional hydrogen bond with CYS A:470 residue,

01 pi-sigma interaction with GLY A:472 residue.

By analyzing those results, it is possible to understand

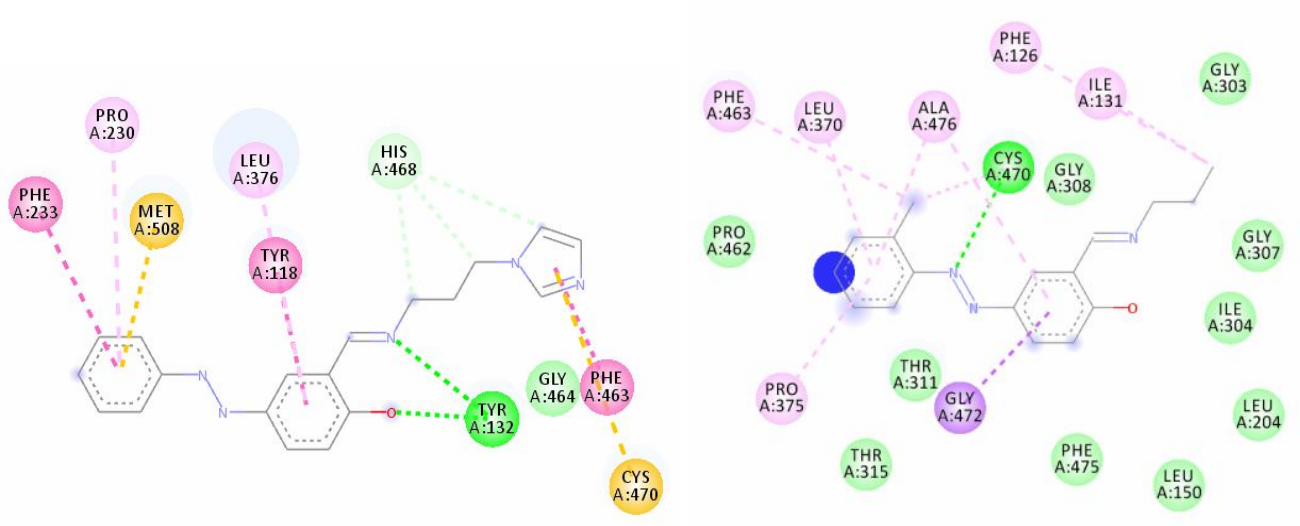

L1 L4

Fig. 4. Interactions between the protein sterol 14 alpha-demethylase and compounds L1 (the more active) and L4 (the less active).

Table 5. Different Types and Number of the Interactions between Molecules L1 and L2 with the Potential Target Sterol-14-Alpha-demethylase

Compounds	Hydrogen bonds (green)		pi-sigma (dark pink)		Pi sulfure (yellow)		Mauve (Pi-alkyle)	
	Number	A.A	Number	A.A	Number	A.A	Number	A.A
L1	3	(2)TYR132His 468	3	PHE463 PHE233 THY118	2	MET508CYS470	2	LEU376 PRO230
L4	1	CYS470	NO		NO		6	ILE131 PHE126 ALA476 LEU370 PHE463 PRO375

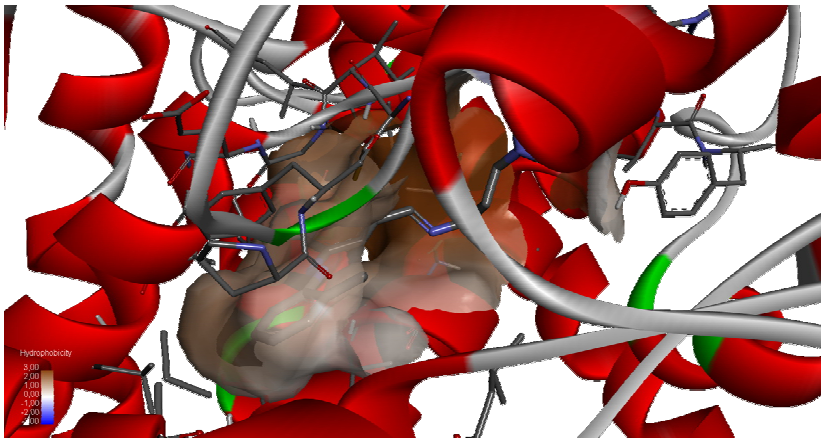

Fig. 5. The hydrophobicity between the most active molecule in solution media (L2) and (CYP51) visualized with Discovery Studio visualizer program.

the difference between the most active L1 and the least active compound L4. Based on the results, the activity difference observed between the most active molecule (L1) and the least active one (L4) can be explained by the difference in the type and the number of different bonds. Indeed, the absence of pi-sigma and pi-Sulfide bonds in the least active molecule may probably explain this difference on the antifungal activity, since these bonds stabilize the molecule in the most active conformation in the binding site, indicating that the several groups in compound L1 (the most active species) presents many more hydrogen bonds and pi-sigma interactions compared to compound L4 (the less active species). Also, the presence of the three hydrogen bonds in the most active molecule may explain the strong antifungal activity. The ligand inhibits the enzyme 14-α-demethylase and probably blocks the synthesis of ergosterol causing then a disturbance in the plasma membrane, followed by cell leakage and eventually death of the pathogen. In a simple way, it gives us an idea about the potential mechanism of action of these molecules. While the other types of binding (for example pi-alkyle interactions) appears to be not very necessary for the biological activity but only for the stability of the ligand.

It should be noted that the L4 molecule does not have an imidazole unit; therefore, the absence of these specific bonds probably leads the low activity observed both in solid state and in solution. Consequently, the presence of imidazole units has a great effect on the activity of the target molecules. This is in a good agreement with the experimental observations in the solid media. However, a certain discrepancy was noted between the obtained results in solid state and those in liquid state; indeed, in liquid medium, high antifungal activities MIC_{80} were observed against *C. albicans* (L1 (0.8 µg ml^{-1}) < L3 (0.2 µg ml^{-1}) < L2 (0.1 µg ml^{-1})). As in the solid state, where the activity is expressed by the diameter of the inhibition zone, L1 possesses important antifungal properties, although they are more interesting in the case of L2 and L3 (L1 (17 mm) < L3 (14.5 mm) = L2 (14.5)) [15]. To explain this phenomenon, we calculated log P, which is proportional to hydrophobicity, for each ligand. This hydrophilic ("water-loving") or hydrophilic gold ("water-fearing") coefficient is useful in estimating the distribution of the target compound in the solvent used. The obtained results show that the compound L2 is the most hydrophobic (logP = 0.94), followed by L3 (logP = 0.86) and L1 (logP = 0.57), explaining the obtained activities in solution (L2 > L3 > L1). Therefore, we confirm that the lipohilic or hydrophobic character of the compounds affects the antifungal activities in liquid medium by modifying their diffusion (Fig. 5).

CONCLUSIONS

The obtained values of E_{HOMO}, E_{LUMO} are (-5.918,

-2.104), (-5.852, -2.114), (-5.799, -2.026) and (-5.718, -1.991) for L1, L2, L3 and L4, respectively. This can explain that the highest activity of L1 is probably due to the low value of the HOMO energy and the high value of the LUMO energy. This is in a good agreement with the experimental observations suggesting the following order of experimental activities L1 > L2 > L3 > L4.

The calculated band gap value indicates that the L1 molecule has a stable structure.

The higher hardness and lower softness value confirm the stability of L1, suggesting that this molecule could have a better performance as a ligand. This is in good agreement with the experimental observations.

The molecular docking analysis was carried out for the ligands L1-L4 with their corresponding proteins. The most active compound L1 presents many hydrogen bonds and pi-sigma interactions compared to the less active compound L4. Also, the presence of the three hydrogen bonds in the most active molecule may explain the strong antifungal activity. Indeed, the absence of pi-sigma and pi-sulfide bonds in the least active molecule may explain this difference on the antifungal activity, since these bonds stabilize the molecule in the most active conformation in the binding site.

ACKNOWLEDGMENTS

We are grateful to the “Association Marocaine des Chimistes Théoriciens” (AMCT) for its pertinent help concerning the programs. This research did not receive any specific funding and it was carried out as part of the preparation of the doctoral theses of the students cited in the article

Competing Interests

The authors declare that they have no competing interests.

REFERENCES

[1] Forte, B.; Malgesini, B.; Piutti, C.; Quartieri, F.; Scolaro, A.; Papeo,G., A submarine journey: The pyrrole imidazole alkaloids. *Mar. Drugs.* **2009**, *7*, 705-53, DOI: 10.3390/md7040705.

[2] Jin, Z., Muscarine, imidazole, oxazole and thiazole alkaloids. *Nat. Prod. Rep.* **2011**, *28*, 1143-1191, DOI: 10.1039/C3NP70006B.

[3] Hill, R. A., Marine natural products. *Annu. Rep. Prog. Chem., Sect. B: Org. Chem.* **2009**, *105*, 150-166, DOI: 10.1039/B822053K.

[4] Aleksandrova, E. V.; Kravchenko, A. N.; Kochergin P. M., Properties of haloimidazoles. *Chem. Heterocycl. Comp.* **2011**, *47*, 261-289, DOI: 10.1007/ s10593-011-0754-8.

[5] Shalini, K.; Sharma, P. K.; Kumar, N., Imidazole and its biological activities: a review. *Der Chem. Sci. Int.* **2013**, *1*, 253-260, DOI: 10.3923/ sciintl.2013.253.260.

[6] Lambardino, J. G.; Wiseman, E. H., Preparation and antiinflammatory activity of some nonacidic trisubstituted imidazoles. *J. Med. Chem.* **1974**, *17*, 1182-1188, DOI: 10.1021/jm00257a011.

[7] Puratchikody, A.; Doble, M., Anti-nociceptive and anti-inflammatory activities and QSAR studies on 2-substituted-4,5-diphenyl-1H-imidazoles. *Bioorg Med Chem.* **2007**, *15*, 1083-90, DOI: 10.1016/ j.bmc.2006.10.025.

[8] Li, Y. F.; Wang, G. F.; Luo, Y.; Huang, W. G.; Tang, W.; Feng, C. L.; Shi, L. P.; Ren, Y.D.; Zuo, J.P.; Lu, W., Identification of 1-isopropylsulfonyl-2-amine benzimidazoles as a new class of inhibitors of hepatitis B virus. *Eur. J. Med. Chem.* **2007**, *42*, 1358-1364, DOI: 10.1016/j.ejmech.2007.03.005.

[9] Ansari, K. F.; Lal, C., Synthesis, physicochemical properties and antimicrobial activity of some new benzimidazole derivatives. *Eur. J. Med. Chem.* **2007**, *42*, 1358-64, DOI: 10.1016/j.ejmech.2007.03.005.

[10] Gomez, H. T.; Nunez, E. H.; Rivera, I. L.; Alverez, J. G.; Rivera, R. C.; Puc, R. M.; Ramos, R. A., Design, synthesis and in vitro antiprotozoal activity of benzimidazole-pentamidine hybrids. *Bioorg. Med. Chem. Lett.* **2008**, *18*, 3147-3151, DOI: 10.1016/ j.bmcl.2008.05.009.

[11] Süleymanoğlu, N.; Ustabaş, R.; Direkel, Ş.; Alpaslan, Y. B.; Ünver, Y., 1,2,4-Triazole derivative with Schiff base; thiol-thione tautomerism, DFT study and antileishmanial activity. *J. Mol. Struct.* **2017**, *1150*, 82-87, DOI: 10.1016/j.molstruc.2017.08.075.

[12] Mihajlovic, M. B. P.; Radovanovic, M. B.; Tasic, Z. Z.; Antonijevic, M. M., Imidazole based compounds as copper corrosion inhibitors in seawater. *J. Mol. Liq*. **2017**, *225*, 127-136, DOI: 10.1016/ j.molliq.2016.11.038.

[13] Qiu, X.; Shi, J.; Xu, X.; Lu, Y.; Sun, Q.; Xue, S.; Yang, W., Tuning the optoelectronic properties of phenothiazine-based D-A-type emitters through changing acceptor pattern, *Dyes Pigm*. **2017**, *147*, 6-15, DOI: 10.1016/j.dyepig.2017.07.064.

[14] Perrier, A.; Jacquemin, D., Theoretical investigation of the photochromic properties of (2.2) paracyclophane-bridged imidazole dimers and bis(imidazole) dimers. *Tetrahedron,* **2017**, *73*, 4936-4949. DOI: 10.1016/j.tet.2017.05.050.

[15] Slassi, S.; Fix-Tailler, A.; Larcher, G.; Amine, A.; El-Ghayoury, A., Imidazole and azo-based schiff bases ligands as highly active antifungal and antioxidant components. *Heteroat. Chem*. **2019**, *2019*, 1-8, DOI: 10.1155/2019/6862170.

[16] Ericsson, J.; Chryssanthou, E.; Klingspor, L.; Johansson, A. G.; Ljungman, P.; Svensson, E., Candidaemia in Sweden: a nationwide prospective observational survey. Clin Microbiol Infect. 2013, 19, 218-21, DOI: 10.1111/1469-0691.12111.

[17] Montagna, M. T.; Lovero, G.; De Giglio, O.; Iatta, R.; Caggiano, G.; Montagna, O.; Laforgia, N., Invasive fungal infections in neonatal intensive care units of Southern Italy: a multicentre regional active surveillance (AURORA project). *J. Prev. Med. Hyg.* **2010**, *51*, 125-130. Wisplinghoff, J.; Ebber, L.; Geurtz, D.; Stefanik, Y.; Major, M. B., Edmond. Nosocomial bloodstream infections due to Candida spp. in the USA: species distribution, clinical features and antifungal susceptibilities.

[18] Wisplinghoff, H.; Ebbers, J.; Geurtz, L.; Stefanik, D.; Major, Y.; Edmond, M. B.; Wenzel, R. P.; Seifert, H., Nosocomial bloodstream infections due to Candida spp. in the USA: Species distribution, clinical features and antifungal susceptibilities. *Int. J. Antimicrob. Agents.* **2014**, *43*, 78-81, DOI: 10.1016/ j.ijantimicag.2013.09.005.

[19] Becke, A. D., Density-functional exchange-energy approximation with correct asymptotic behavior. *Phys. Rev. A*. **1988**, *38*, 3098-3100, DOI: org/10.1103/ PhysRevA.38.3098.

[20] Pihet, M.; Carrere, J.; Cimon, B., Occurrence and relevance of filamentous fungi in respiratory secretions of patients with cystic fibrosis-A review. *Med. Mycol.* **2009**, *47*, 387-397, DOI: 10.1080/ 13693780802609604.

[21] Lee, C.; Yang, W.; Parr, R. G., Development of the Colle-Salvetti correlation-energy formula into functional of the electron density. *Phys. Rev. B.* **1988**, *37*, 785-789, DOI: 10.1103/PhysRevB.37.785.

[22] Frisch, M. J.; Trucks, G. W.; Schlegel, H. B.; Scuseria, G. E.; Robb, M. A.; Cheeseman, J. R.; Scalmani, G.; Barone, V.; Mennucci, B.; Petersson, G. A.; Nakatsuji, H.; Caricato, M.; Li, X.; Hratchian, H. P.; Izmaylov, A. F.; Bloino, J.; Zheng, G.; Sonnenberg, J. L.; Hada, M.; Ehara, M.; Toyota, K.; Fukuda, R.; Hasegawa, J.; Ishida, M.; Nakajima, T.; Honda, Y.; Kitao, O.; Nakai, H.; Vreven, T.; Montgomery, J. A.; Jr.;. Peralta, J. E.; Ogliaro, F.; Bearpark, M.; Heyd, J. J.; Brothers, E.; Kudin, K. N.; Staroverov, V. N.; Kobayashi, R.; Normand, J.; Raghavachari, K.; Rendell, A.; Burant, J. C.; Iyengar, S. S.; Tomasi, J.; Cossi, M.; Rega, N.; Millam, J. M.; Klene, M.; Knox, J. E.; Cross, J.B.; Bakken, V.; Adamo, C.; Jaramillo, J.; Gomperts, R.; Stratmann, R. E.; Yazyev, O.; Austin, A. J.; Cammi, R.; Pomelli, C.; Ochterski, J. W.; Martin, R. L.; Morokuma, K.; Zakrzewski, V. G.; Voth, G. A.; Salvador, P.; Dannenberg, J. J.; Dapprich, S.; Daniels, A. D.; Farkas, Ö.; Foresman, J. B.; Ortiz, J. V.; Cioslowski, J.; Fox, D. J., Gaussian, Inc. Wallingford CT, 2009.

[23] Jacquemin, D.; Wathelet, V.; Perpete, E. A.; Adamo C., Extensive TD-DFT benchmark: singlet-excited states of organic molecules. *J. Chem. Theory Comput.* **2009**, *8*, 5, 2420-35, DOI: 10.1021/ct900298e.

[24] Ayachi, S.; Bouzakraoui, S.; Hamidi, M.; Bouachrine, M.; Molinié, P.; Alimi, K., Prediction of electropolymerization mechanisms of two substituted phenylene: Poly–3-methoxy-toluenes (P3mt1 and P3mt2). *J. Appl. Polym. Sci.* **2006**, *100*, 57-64, DOI: 10.1002/app.22640.

[25] Bouachrine, M.; Bouzakraoui, S.; Hamidi, M.; Ayachi, S.; Alimi, K.; LèrePorte, J. -P.; Moreau, J.,

Synthesis and characterization of co-polymers involving various thiophene and phenylene monomers. *Synth. Met.* **2004**, *145*, 237-243. DOI: 10.1016/j.synthmet.2004.05.008.

[26] Bourass, M.; Benjelloun, A. T.; Benzakour, M.; Mcharfi, M.; Hamidi, M.; Bouzzine, S. M.; Bouachrine, M., DFT and TD-DFT calculation of new thienopyrazine-based small molecules for organic solar cells. *Chem. Cent. J.* **2016**, *10*, 67, DOI: 10.1186/s13065-016-0216-6.

[27] Ayachi, S.; Alimi, K.; Bouachrine, M.; Hamidi, M.; Mevellec, J. Y.; Lère-Porte J. P., Spectroscopic investigations of copolymers incorporating various thiophene and phenylene monomers, *Synth. Met.,* **2006**, *156*, 318-326, DOI: 10.1016/ j.synthmet.2005.12.010.

[28] ElKhattabi, S.; Fitri, A.; Benjelloun, A. T.; Benzakour, M.; Mcharfi, M.; Hamidi, M.; Bouachrine, M., Theoretical investigation of electronic, optical and photovoltaic properties of alkylamine-based organic dyes as sensitizers for application in DSSCs. *J. Mater. Environ. Sci.* **2018**, *9*, *3*, 841-853, DOI: 10.26872/jmes.2018.9.3.93.

[29] Yanai, T.; Tew, D. P.; Handy. N. C., A new hybrid exchange-correlation functional using the Coulomb-attenuating method (CAM-B3LYP). *Chem. Phys. Lett.* **2004**, *393*, 51-56, DOI: 10.1016/j.cplett.2004.06.011.

[30] Morris, G. M.; Goodsell, D. S.; Halliday, R. S.; Huey, R.; Hart, W. E.; Belew, R. K.; Olson, A. J., Automated docking using a Lamarckian genetic algorithm and an empirical binding free energy function. *J. Comput. Chem.* **1998**, *19*, 1639-1662, DOI: 10.1002/(SICI)1096-987X(19981115)19:14<1639::AID-JCC10>3.0.CO;2-B.

[31] Trott, O.; Olson, A. J., AutoDock Vina: improving the speed and accuracy of docking with a new scoring function, efficient optimization, and multithreading, *J. Comput. Chem.* **2010**, *31*, 455-461, DOI: 10.1002/ jcc.21334.

[32] Dassault Systèmes BIOVIA Discovery Studio Modeling Environment, Release 2017 Dassault Systèmes, 2016. http://accelrys.com/products/ collaborative-science/biovia-discovery-studio/.

[33] Lepesheva, G. I.; Waterman, M. R., Sterol 14alpha-demethylase cytochrome P450 (CYP51), a P450 in all biological kingdoms. *Biochim. Biophys. Acta.* **2007**, **1770**, *3*, 467-77, DOI: 10.1016/j.bbagen.2006.07.018.

[34] Slassi, S.; Aarjane, M.; Amine, A.; Zouihri, H.; Yamni, K., 2-((E)-[3-(1H-Imidazol-1-yl)prop-yl]iminomethyl)-4-[(E)-(2-methylphenyl)diazen-yl]phenol. *IUCrData,* **2017**, *2*, x171477.

[35] Morrison, R. C., The extended Koopmans' theorem and its exactness. *J. Chem. Phys.* **1992**, *96*, 3718, DOI: 10.1063/1.461875.

[36] Wang, H.; Wang, X.; Wang, H.; Wang, L.; Liu, A., DFT study of new bipyrazole derivatives and their potential activity as corrosion inhibitors. *J. Mol. Model.* **2007**, *13*, 147-153, DOI: 10.1007/s00894-006-0135-x.

[37] Kikuchi, O.; Hesketh, G.; Clayworth, D., Novel method for the display of multivariate data using neural networks. *J. Mol. Graph.* **1991**, *9*, 115-118, DOI: 10.1016/0263-7855(91)85008-M.

[38] Metabocard for 4,4-Dimethylcholesta-8,14,24-trienol (HMDB01023), Human Metabolome Database, February 2014.

[39] Lepesheva, G. I.; Waterman, M. R., Sterol 14alpha-demethylase cytochrome P450 (CYP51), a P450 in all biological kingdoms. *Biochim. Biophys. Acta.* **2007**, *1770*, 467-77, DOI: 10.1016/j.bbagen.2006.07.018.

[40] Lamb, D. C.; Kelly, D. E.; Baldwin, B. C.; Gozzo, F.; Boscott, P.; Richards, W. G.; Kelly, S. L., Differential inhibition of Candida albicans CYP51 with azole antifungal stereoisomers. *FEMS Microbiol. Lett.* **1997**, *149*, 25-30. DOI:10.1111/j.1574-6968.1997.tb10303.x.

[41] Hargrove, T. Y.; Friggeri, L.; Wawrzak, Z.; Qi, A.; Hoekstra, W. J.; Schotzinger, R. J.; York, J. D.; Guengerich, F. P.; Lepesheva, G. I., Structural analyses of candida albicans sterol 14α-demethylase complexed with azole drugs address the molecular basis of azole-mediated inhibition of fungal sterol biosynthesis. *J. Biol. Chem.* **2017**, *21*, 292, 6728-6743, DOI: 10.1074/jbc.M117.778308.